



**HAL**  
open science

# Low-Frequency MEMS Electrostatic Vibration Energy Harvester With Corona-Charged Vertical Electrets and Nonlinear Stoppers

Y Lu, F Cottone, S Boisseau, Dimitri Galayko, Frédéric Marty, Philippe Basset

► **To cite this version:**

Y Lu, F Cottone, S Boisseau, Dimitri Galayko, Frédéric Marty, et al.. Low-Frequency MEMS Electrostatic Vibration Energy Harvester With Corona-Charged Vertical Electrets and Nonlinear Stoppers. The 15th International Conference on Micro and Nanotechnology for Power Generation and Energy Conversion Applications (PowerMEMS 2015), Dec 2015, Boston, United States. pp.012003, 10.1088/1742-6596/660/1/012003 . hal-01270683

**HAL Id: hal-01270683**

**<https://hal.sorbonne-universite.fr/hal-01270683>**

Submitted on 8 Feb 2016

**HAL** is a multi-disciplinary open access archive for the deposit and dissemination of scientific research documents, whether they are published or not. The documents may come from teaching and research institutions in France or abroad, or from public or private research centers.

L'archive ouverte pluridisciplinaire **HAL**, est destinée au dépôt et à la diffusion de documents scientifiques de niveau recherche, publiés ou non, émanant des établissements d'enseignement et de recherche français ou étrangers, des laboratoires publics ou privés.



Distributed under a Creative Commons Attribution 4.0 International License

## Low-Frequency MEMS Electrostatic Vibration Energy Harvester With Corona-Charged Vertical Electrets and Nonlinear Stoppers

This content has been downloaded from IOPscience. Please scroll down to see the full text.

2015 J. Phys.: Conf. Ser. 660 012003

(<http://iopscience.iop.org/1742-6596/660/1/012003>)

View [the table of contents for this issue](#), or go to the [journal homepage](#) for more

Download details:

IP Address: 134.157.80.136

This content was downloaded on 08/02/2016 at 11:57

Please note that [terms and conditions apply](#).

# Low-Frequency MEMS Electrostatic Vibration Energy Harvester With Corona-Charged Vertical Electrets and Nonlinear Stoppers

Y Lu<sup>1</sup>, F Cottone<sup>1,2</sup>, S Boisseau<sup>3</sup>, D Galayko<sup>4</sup>, F Marty<sup>1</sup>, P Basset<sup>1</sup>

<sup>1</sup>Université Paris-Est / ESYCOM / ESIEE Paris, France

<sup>2</sup>Now at University of Perugia, NIPS Laboratory, Department of Physics, Italy

<sup>3</sup>CEA, Leti, Minatec Campus, Grenoble, France

<sup>4</sup>UPMC-Sorbonne Universités / LIP6, CNRS, France

E-mail: yingxian.lu@esiee.fr

**Abstract.** This paper reports for the first time a MEMS electrostatic vibration energy harvester (e-VEH) with corona-charged vertical electrets on its electrodes. The bandwidth of the 1-cm<sup>2</sup> device is extended in low and high frequencies by nonlinear elastic stoppers. With a bias voltage of 46 V (electret@21 V + DC external source@25 V) between the electrodes, the RMS power of the device reaches 0.89  $\mu$ W at 33 Hz and 6.6  $\mu$ W at 428 Hz. The -3dB frequency band including the hysteresis is 223~432 Hz, the one excluding the hysteresis 88~166 Hz. We also demonstrate the charging of a 47  $\mu$ F capacitor used for powering a wireless and autonomous temperature sensor node with a data transmission beyond 10 m at 868 MHz.

## 1. Introduction

It is widely admitted that low-frequency vibrations naturally exist in the environment and that they offer a potential resource of energy to power electronic devices or sensors. However, the efforts are always faced with the difficulty to capture low-frequency vibration energy with MEMS-based VEHs. Confined by the miniature size of the MEMS VEHs, the maximum displacement of the movable part is limited within the void space in the device, and the mass in the resonant structure is limited by its volume, which both limit the power of the device in low frequency. By using nonlinear soft springs, the operating frequency bandwidth is expanded at low frequencies [1], but the use of polymers in the device adds complexity to the fabrication process.

In this work we present a MEMS e-VEH with a large frequency bandwidth, effective from 50 Hz and obtained by the use of nonlinear external stoppers in silicon. In addition, although only soft x-ray and UV charging had been proposed as charging methods for MEMS vertical electrets [2], we demonstrate that it is also possible with a classical point-grid-plane triode Corona charging method.

## 2. Device Description and Fabrication

A simplified schematic of the prototype is shown in Figure 1. A moving silicon proof mass (400  $\mu$ m-thick) is connected to fixed ends by linear serpentine springs. On both ends of the movable mass, stoppers standing against clamped-clamped elastic beams have been added [3]. At sufficient acceleration levels, the stoppers on the ends of the movable mass hit the elastic beams, which deforms them; this results in a low-frequency and a wideband response of the device.



The fabrication process is derived from [4]. The silicon layer is patterned with an Al mask using a DRIE process, and is anodically bonded with a glass substrate. A layer of parylene is deposited all over the device. The parylene layer on the movable part is negatively charged with the corona charging setup while the parylene layer on the fixed electrodes is not charged.

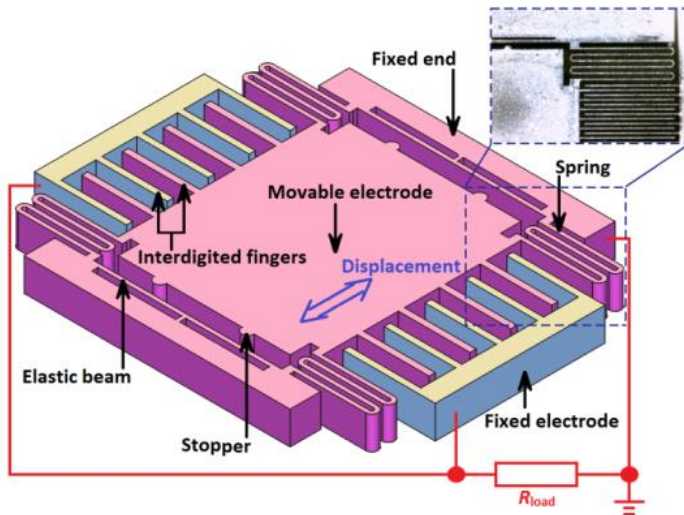


Figure 1. Simplified schematic of the silicon layer of the electrostatic energy harvester. The nonlinear spring system consists of the linear serpentine springs and the nonlinear elastic beams standing against stoppers.

### 3. Device Characterization

#### 3.1. Built-in voltage measurement

In order to measure the built-in bias voltage ( $V_{\text{bias}}$ ) provided by the electret, we propose to use the circuit shown in Figure 2(a). The saturation value of the voltage across the storage capacitor  $C_v$  is given by:

$$V_{\text{store}} = V_{\text{bias}} \left( 1 - \frac{C_{\text{min}}}{C_{\text{max}}} \right)$$

where  $C_{\text{min}}$  and  $C_{\text{max}}$  are the minimum and the maximum values of the variable capacitance  $C_{\text{var}}$ . The saturation value of  $V_{\text{store}}$  is 11 V as given by the measurement shown in Figure 2(b), and the measurement of capacitance  $C_{\text{var}}$  indicates a minimum of 50 pF and a maximum of 105 pF respectively. Thus, the internal voltage provided by the electret is about  $V_{\text{bias}} = 21$  V.

However, the device could stand for much higher bias voltage. In order to fully demonstrate the capability of the prototype, we also performed experiments with an additional DC bias at 25 V in series with the prototype to investigate its performance with a higher voltage bias (up to 46 V).

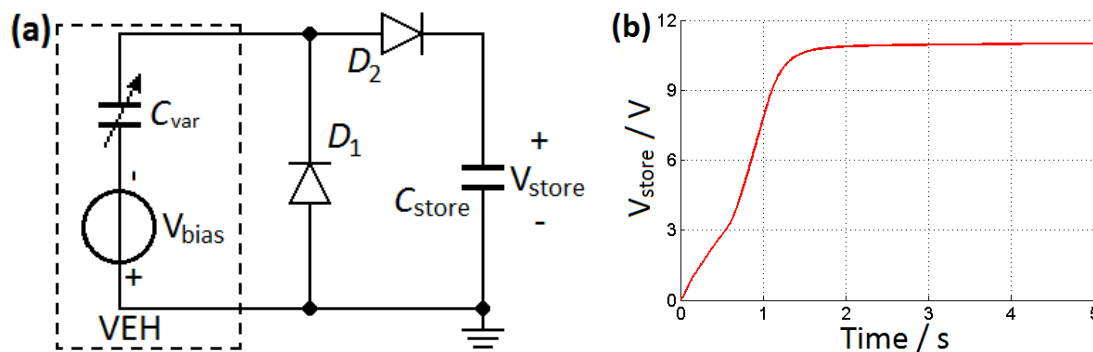


Figure 2 (a). Circuit for built-in voltage measurement of the electret layer, where  $C_{\text{store}}=1.1$  nF; (b). Evolution of  $V_{\text{store}}$  at 2.0  $g_{\text{RMS}}$ , 145 Hz.

### 3.2. Characterization of the performance in frequency domain

The device is connected in series with a load resistor of  $6.65 \text{ M}\Omega$  and is subjected to power measurement with frequency sweeping. The device is firstly tested at  $0.1 g_{\text{RMS}}$  for the natural frequency measurement  $f_0$ , which is observed at  $f_0 = 104 \text{ Hz}$ .

Figure 3 gives the RMS power against the frequency at higher accelerations ( $0.5$  and  $2.0 g_{\text{RMS}}$ ). Typical spring stiffening effects and hysteresis are observed, which is caused by the impacts between the stoppers and the nonlinear elastic beams.

With the bias voltage of  $21 \text{ V}$  (electret alone), the maximum output power at  $0.5 g_{\text{RMS}}$  is  $0.48 \mu\text{W}$ , and the one at  $2.0 g_{\text{RMS}}$  reaches  $1.3 \mu\text{W}$ . If the hysteresis is excluded, the maximum power at  $0.5 g_{\text{RMS}}$  is  $0.2 \mu\text{W}$ , while it reaches  $0.4 \mu\text{W}$  at  $2.0 g_{\text{RMS}}$ . An output power of at least  $0.1 \mu\text{W}$  can be harvested within the  $45\sim 450 \text{ Hz}$  frequency band including the hysteresis frequency span.

With a higher bias voltage of  $46 \text{ V}$  (electret at  $21 \text{ V}$  and external DC bias at  $25 \text{ V}$ ), both the power and the bandwidth of the device are improved. The power reaches  $1 \mu\text{W}$  at  $0.5 g_{\text{RMS}}$  just below the frequency span of hysteresis, and reaches  $2.1 \mu\text{W}$  at  $161 \text{ Hz}$ . At  $2.0 g_{\text{RMS}}$ , the power reaches  $6.6 \mu\text{W}$  at  $428 \text{ Hz}$ , and the power before reaching hysteresis is  $2.4 \mu\text{W}$ . Within the frequency range of  $29\sim 432 \text{ Hz}$ , the output power is superior to  $0.6 \mu\text{W}$ . Finally, the  $-3 \text{ dB}$  frequency bands with and without hysteresis are  $223\sim 432 \text{ Hz}$  and  $88\sim 166 \text{ Hz}$ , respectively.

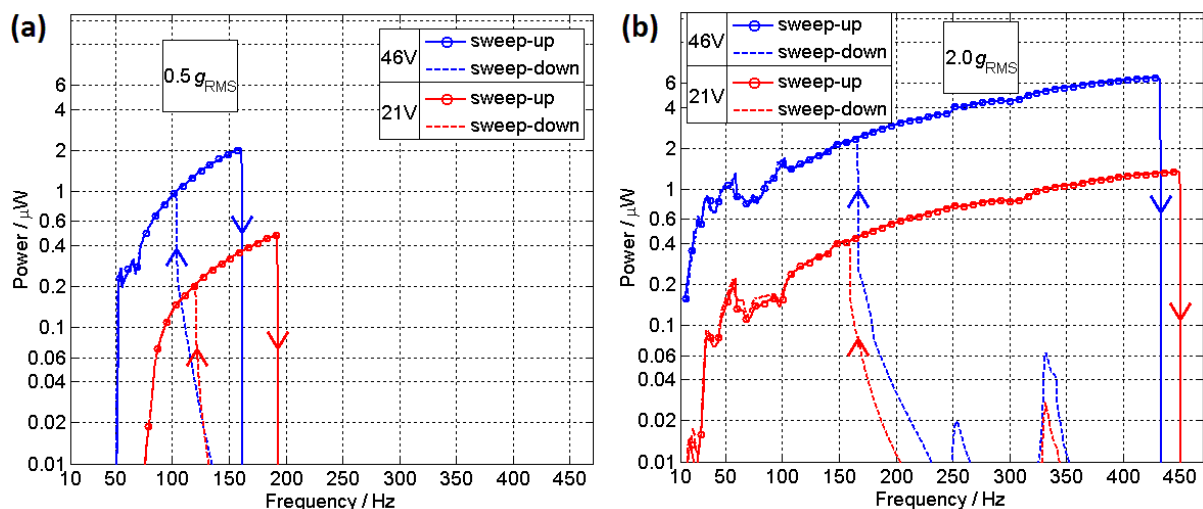


Figure 3. RMS output power vs. frequency for bias voltages of  $21 \text{ V}$  (electret alone) and  $46 \text{ V}$  (electret@ $21\text{V}$  + DC external bias@ $25\text{V}$ ) at  $0.5 g_{\text{RMS}}$  (a) and  $2.0 g_{\text{RMS}}$  (b),  $R_{\text{load}}=6.65 \text{ M}\Omega$ .

### 3.3. Powering sensors and wireless data transmission

The power supply of a wireless temperature sensor node supplied by our energy harvester is shown in Figure 4(a). The output power of the device without any additional DC bias (electret alone –  $V_{\text{bias}} = 21 \text{ V}$ ) is rectified with a diode bridge, and stored in a  $47\text{-}\mu\text{F}$  capacitor. This capacitor powers a low-power sensor node made of a temperature sensor, a MSP430 microcontroller and a RF chip working at  $868 \text{ MHz}$  (CC430). A low-power Schmitt trigger (Switch module) [5] is used to detect when enough energy has been stored in the capacitor to supply the wireless sensor node. The Switch module reads the voltage across  $C_s$  ( $U_{C_s}$ ) and closes the switch to supply the wireless sensor node as soon as  $U_{C_s}$  reaches  $3.8 \text{ V}$ . The switch is re-opened when  $U_{C_s}$  falls below  $2.8 \text{ V}$  in order not to uselessly discharge  $C_s$ . The power consumption of the switch module is lower than  $40 \text{ nA}$  at  $3 \text{ V}$ . A photograph of the experimental setup is also shown in Figure 4(b).

Figure 4(c) shows the voltage evolution during a series of data transmission experiment. The storage capacitor  $C_s$  is charged with the e-VEH prototype working at  $300 \text{ Hz}$  with an acceleration of

2.0  $g_{RMS}$ . The initial voltage across  $C_s$  rises from 0 V to 3.8 V in 7.2 min. This corresponds to a stored energy of 334  $\mu\text{J}$ ; then, the average harvested power stored in  $C_s$  is 0.77  $\mu\text{W}$ .  $U_{Cs} = 3.8$  V is detected by the Schmitt trigger which closes the switch (PMOS transistor) to supply the wireless sensor node. The wireless sensor wakes up, performs its temperature measurement and sends the information wirelessly. This operation occurs twice each time the sensor node is turned on. The voltage drop for a measurement and a transmission up to 10 m is 0.7 V, which corresponds to an energy consumption of 102  $\mu\text{J}$  (155  $\mu\text{J}$  for two successive measurements and RF emissions). Finally, it takes about 2 min to recharge  $C_s$  from 2.8 V to 3.8 V, which corresponds to an average harvested power of 1.27  $\mu\text{W}$ . Then, a new measurement cycle (2 measures and 2 data emissions) restarts... and so on.

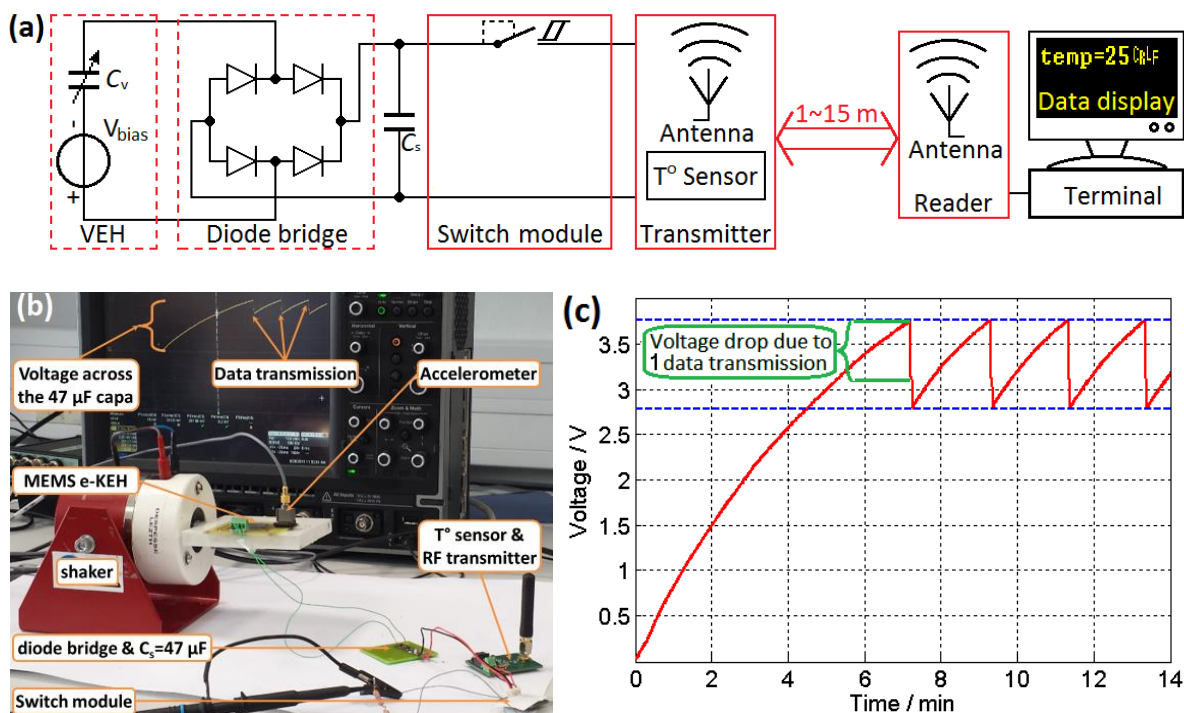


Figure 4 (a). Schematic and (b). photograph of the experiment of data transmission; (c). voltage evolution on  $C_s$  with time during the experiment.

#### 4. Conclusion

We have reported on a low-frequency and large bandwidth 1-cm<sup>2</sup> silicon-based e-VEH prototype with Corona-charged vertical electrets and nonlinear external stoppers. The device has been connected to a diode-bridge capacitor circuit to supply a wireless sensor node based on a CC430 chip with an emission of a temperature measurement every 2 minutes.

#### Acknowledgments

This work is sponsored by the *SATT-IDFINNOV*.

#### References

- [1] D. Miki, M. Honzumi, Y. Suzuki, et al, *Proc. of IEEE MEMS'10*, pp. 176-179, 2010
- [2] Y. Suzuki, *IEEJ Trans. Electrical & Electronic Eng.* **6** pp 101-111, 2011
- [3] F. Cottone, P. Basset, F. Marty, et al, *Proc. of IEEE MEMS'14*, pp. 385-388, 2014
- [4] Basset P, Galayko D, Cottone F, et al. *J. Micromech. & Microeng.*, **24** 035001, 2014
- [5] STMicroelectronics/CEA Patent pending